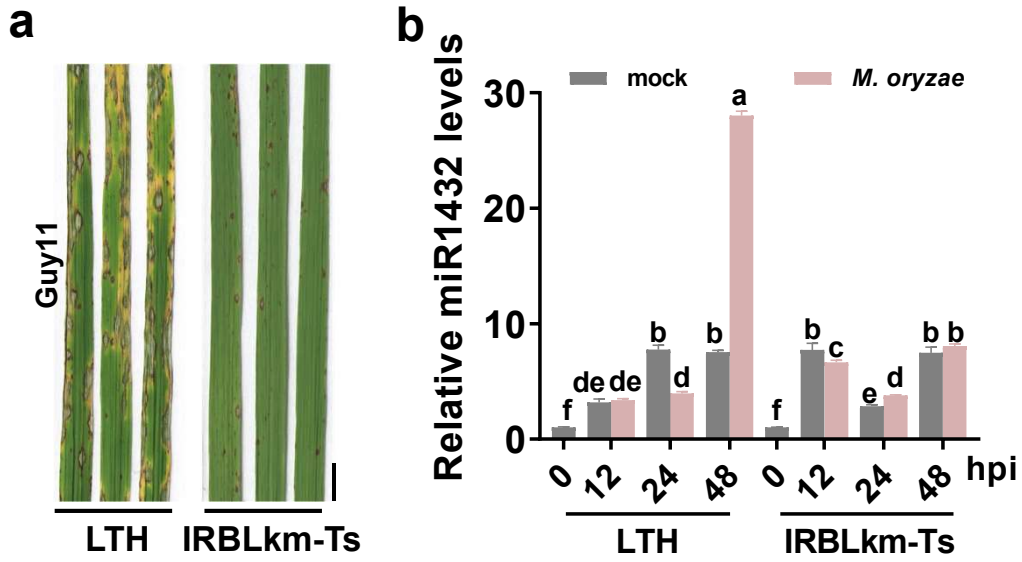

Additional file 1: Figure S1. Rice miR1432 is responsive to blast fungus. **a** The disease lesions on leaves of LTH and IRBLkm-Ts with the inoculation of *Magnaporthe oryzae* strain Guy11. The photo was captured five days post-inoculation. **b** The Reverse transcription-quantitative polymerase chain reaction (RT-qPCR) data show miR1432 levels in LTH and IRBLkm-Ts with or without Guy11 treatment. Data are shown as mean ± SD (n= 3 independent samples). Different letters above the bars show significant differences ($P < 0.01$) as determined by the One-way Tukey-Kramer test. These experiments were repeated two times with similar results.

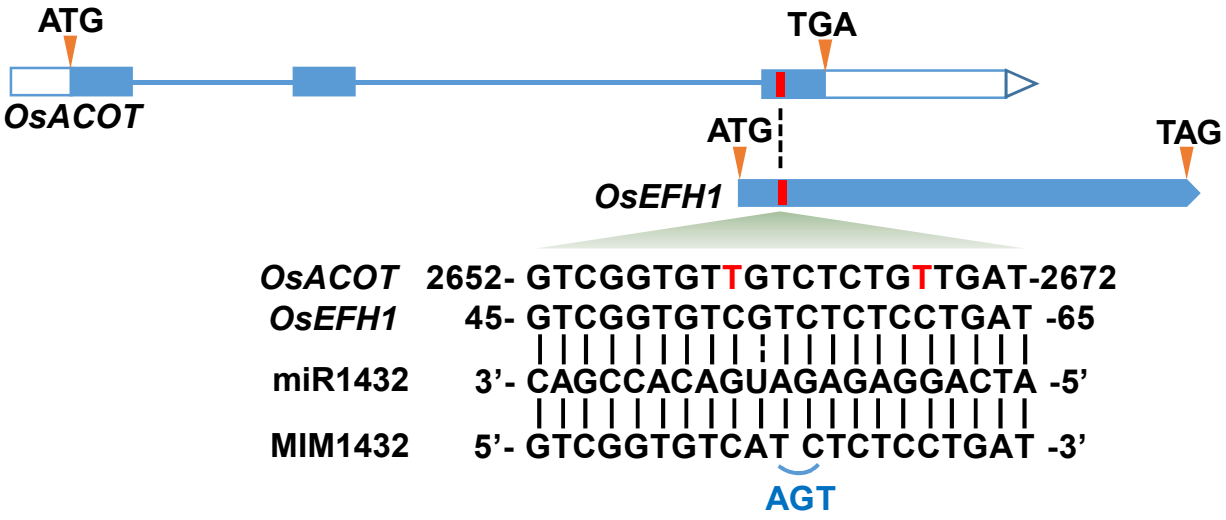

Additional file 2: Figure S2. miR1432 is predicted to target *OsEFH1* and *OsACOT*. The sequence alignment of miR1432, MIM1432, and the target sites of the predicted target genes. Mismatched nucleotides were highlighted in red colors.

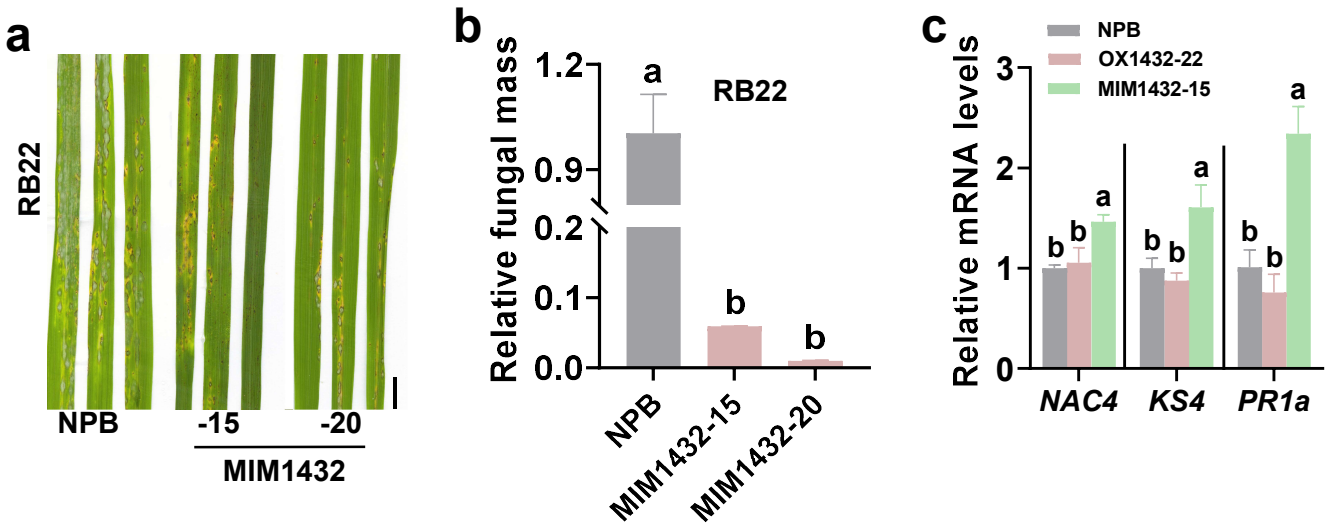

Additional file 3: Figure S3. miR1432 regulates rice resistance to *Magnaporthe oryzae*. **a** The disease phenotypes on leaves of MIM1432 and the Nipponbare control following spray-inoculation with *M. oryzae* strain Guy11. The phenotype was captured five days post-inoculation. Bar= 5 mm. **b** Quantification analysis of the fungal biomass in a. The relative fungal biomass was measured by using the ratio of DNA level of *M. oryzae MoPot2* genes against the rice genomic *ubiquitin* DNA level. The rice *ubiquitin* gene was used as the internal reference gene. **c** The mRNA levels of the defense-related genes in OX1432, MIM1432, and the Nipponbare control 12 hours post-inoculation. For b and c, error bars indicate SD (n = 3 independent samples). Different letters above the bars indicate a significant difference ($P < 0.01$) as determined by a one-way Tukey-Kramer analysis. Similar results were obtained in at least two independent experiments.

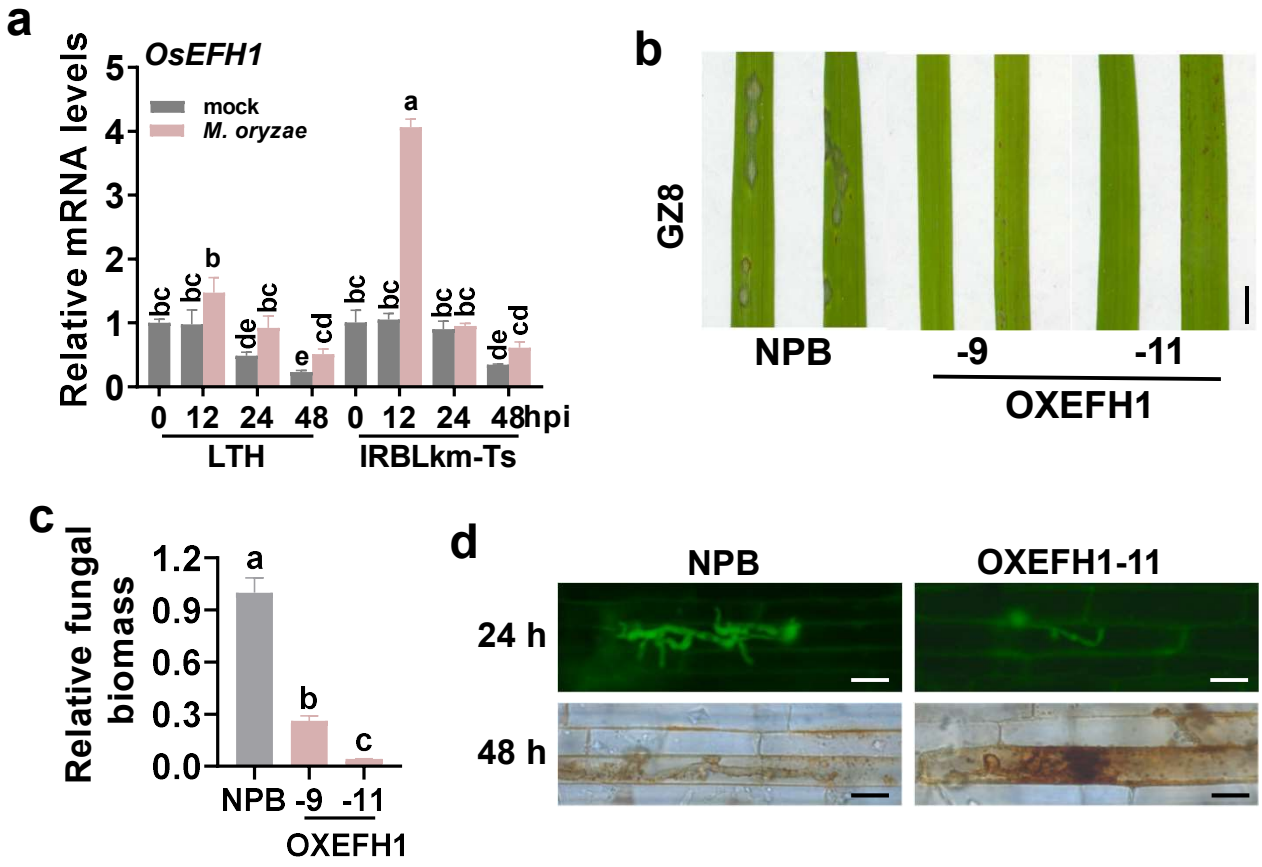

Additional file 4: Figure S4 Overexpression of *OsEFH1* enhances rice blast disease resistance. **a** The reverse transcription-quantitative polymerase chain reaction (RT-qPCR) data show the mRNA levels of *OsEFH1* in LTH and IRBLkm-Ts with or without Guy11 treatment. **b** The disease phenotypes on leaves of OXEFH1 and the Nipponbare control following spray-inoculation of *M. oryzae* strain GZ8 five days post-inoculation. Bars = 5 mm. **c** Quantification analysis of the fungal biomass in b. The relative fungal biomass was measured by using the ratio of DNA level of *M. oryzae Pot2* genes against the rice genomic *ubiquitin* DNA levels. **d** The invasion process of GZ8 at 24 hours post-inoculation (hpi) and the H_2O_2 accumulation at 48 hpi in the invasive sheath cells of OXEFH1 and the Nipponbare control. Bars= 40 μm. For a and c, data are shown as mean ± SD (n= 3 independent samples). Different letters above the bars show significant differences ($P < 0.01$) as determined by the One-way Tukey-Kramer test. Similar results were obtained in at least two independent experiments.

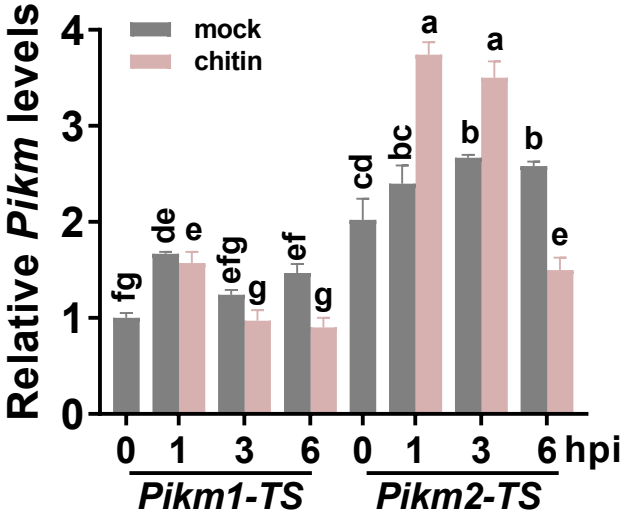

Additional file 5: Figure S5. Chitin regulates the expression of *Pikm* genes in IRBLkm-Ts. The reverse transcription-quantitative polymerase chain reaction (RT-qPCR) data show the mRNA levels of *Pikm1-Ts* and *Pikm2-Ts* in IRBLkm-Ts with or without chitin treatment. Data are shown as mean ± SD (n= 3 independent samples).

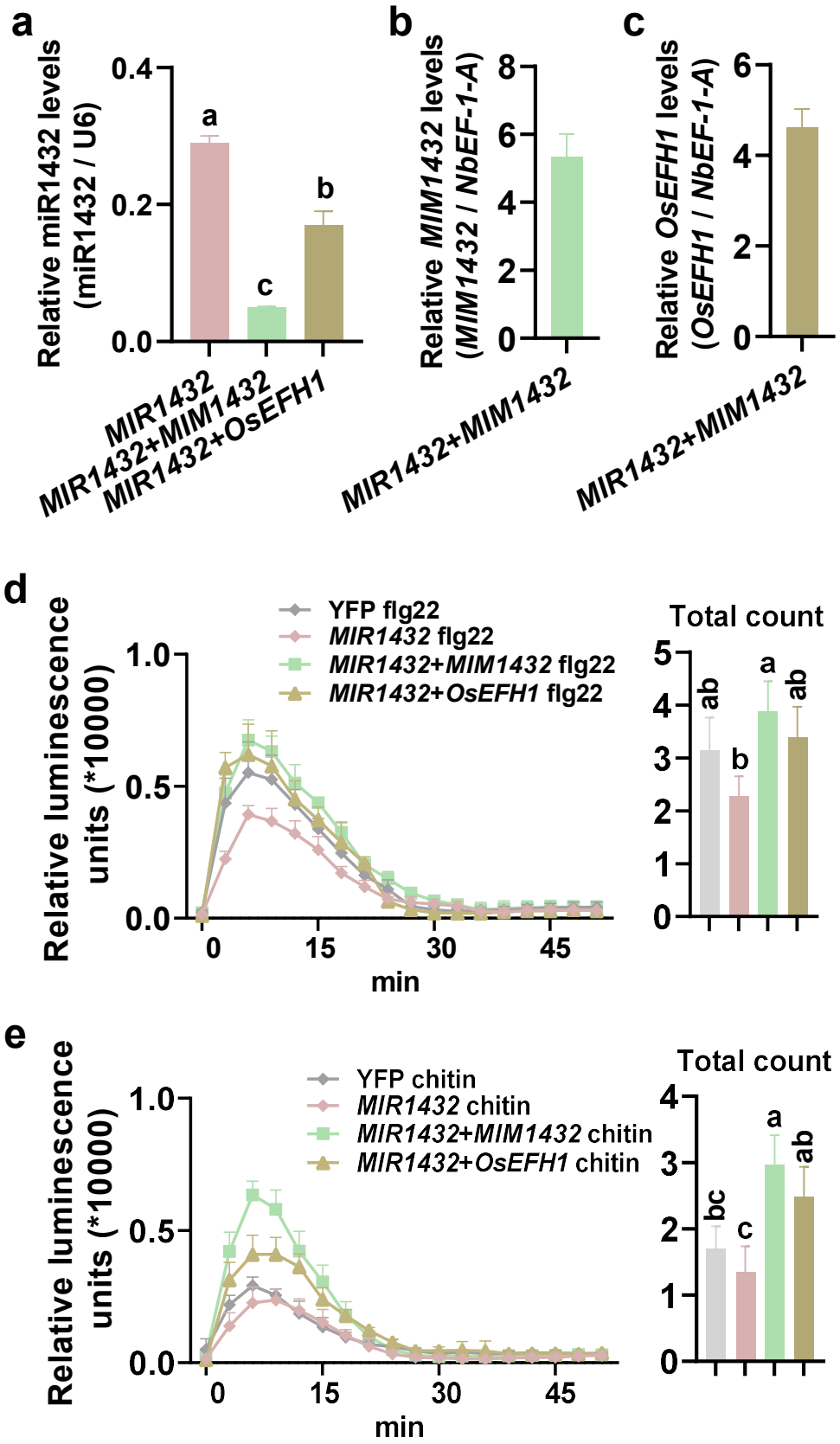

Additional file 6: Figure S6. The miR1432-*OsEFH1* module regulates PAMPs-induced burst of reactive oxidative species (ROS). **a-c** The relative miR1432 levels, *MIM1432* levels, and mRNA levels of *OsEFH1* in the leaves transiently expressing *MIR1432* with or without *MIM1432* or *OsEFH1*, respectively. **d** and **e** The burst of ROS induced by flg22 (d) and chitin (e) in the leaves of *Nicotiana benthamiana* transiently expressing miR1432 with or without MIM1432 or *OsEFH1*, respectively. The leaves transiently expressing YFP are used as the control. Data are shown as mean ± SD (n= 4 independent repeats). Similar results were obtained in at least two independent experiments.